JOURNAL OF FORENSIC SCIENCES

J Forensic Sci, March 2012, Vol. 57, No. 2
doi: 10.1111/j.1556-4029.2011.01971.x
Available online at: onlinelibrary.wiley.com

PAPER

ANTHROPOLOGY

Won-Joon Lee,[1] *M.Sc.; Caroline M. Wilkinson,*[1] *Ph.D.; and Hyeon-Shik Hwang,*[2] *Ph.D.*

An Accuracy Assessment of Forensic Computerized Facial Reconstruction Employing Cone-Beam Computed Tomography from Live Subjects

ABSTRACT: The utilization of 3D computerized systems has allowed more effective procedures for forensic facial reconstruction. Three 3D computerized facial reconstructions were produced using skull models from live adult Korean subjects to assess facial morphology prediction accuracy. The 3D skeletal and facial data were recorded from the subjects in an upright position using a cone-beam CT scanner. Shell-to-shell deviation maps were created using 3D surface comparison software, and the deviation errors between the reconstructed and target faces were measured. Results showed that 54%, 65%, and 77% of the three facial reconstruction surfaces had <2.5 mm of error when compared to the relevant target face. The average error for each reconstruction was −0.46 mm (SD = 2.81) for A, −0.31 mm (SD = 2.40) for B, and −0.49 mm (SD = 2.16) for C. The facial features of the reconstructions demonstrated good levels of accuracy compared to the target faces.

KEYWORDS: forensic science, forensic facial reconstruction, accuracy, 3D computerized modeling method, cone-beam CT, Korean

Forensic (cranio-) facial reconstruction (FFR) is a technique based on both scientific standards and artistic skill to rebuild a face onto a skull to recreate the antemortem appearance of the individual in order to recognize and identify the decedent. It is also known as "forensic facial approximation" (1,2). FFR may be very useful in forensic investigations where other approaches are not possible, or few clues are remaining to aid the identification of human remains. As the public are fascinated with the facial appearance of our ancestors or historically important figures, FFR is also utilized in archaeological research particularly where there are no portraits or sculptures available (3).

It is widely accepted that the first scientific facial reconstruction was attempted by the Swiss-born German anatomist Wilhelm His in 1895 (4,5). He applied average tissue depth thicknesses measured from German cadavers to reconstruct the face of the composer Johann Sebastian Bach. At the turn of the 20th century and for the next few decades, the early techniques of facial reconstruction were mainly applied to archaeological investigations (6). In the former Soviet Union, the renowned archaeologist and anthropologist Mikhail Gerasimov was a pioneer in the field of FFR, and he reconstructed numerous faces for research purposes and forensic identifications (7). In the United States, it was not until 1946 that facial reconstruction was studied, when the anthropologist Wilton Krogman became interested in the procedure and performed research into the accuracy (8). The techniques for reconstructing faces were then employed for the identification of unknown human remains (6) and were ultimately developed as a useful forensic identification tool.

Currently, two basic techniques are utilized in FFR: two-dimensional (2D) and three-dimensional (3D) facial reconstruction. Each technique might be also subdivided into two methods: manual and computerized methods (9,10). The 3D manual methods that have been mainly employed in forensic or archaeological facial reconstruction cases include the anatomical (Russian), anthropometrical (American), and combination (Manchester or British) methods, which were developed by Gerasimov, Krogman, and Neave, respectively (5,11–13). Whatever the techniques applied to the FFR, these 3D manual methods share the common principle of the relationship between the facial skeleton structure and the overlying soft tissue.

It is important for forensic investigation and academic theory to establish the accuracy of the process of facial reconstruction in relation to facial morphology prediction, as facial resemblance is related to recognition. A number of accuracy studies using traditional 3D manual methods have demonstrated good levels of likeness to the target faces (5,14–18). However, some researchers have criticized the 3D manual methods as being highly subjective, time-consuming, requiring artistic intuition, and producing a single-facial estimation (19,20). In an attempt to overcome these limitations, automated FFR methods have been developed (21,22). The concept of the automated, computerized FFR originated from a system for the simultaneous visualization of soft and hard tissues in the field of maxillofacial surgery. Moss et al. (23,24) at the University College London developed a computerized system using a laser line scanner.

Automated 3D computerized FFR commonly fits an "average" face template to a target skull using either a "sparse approach" based on a set of anatomical landmarks placed on the face template or a "dense approach" based on a spatial volumetric template from

[1]Centre for Anatomy and Human Identification, College of Life Sciences, University of Dundee, CAHID, MSI Building, Dow Street, Dundee, DD1 5EH, U.K.
[2]Department of Orthodontics, School of Dentistry, Chonnam National University, Gwangju 500-757, Republic of Korea.

Received 9 Sept. 2010; and in revised form 16 Dec. 2010; accepted 30 Dec. 2010.

both the face and skull (25). The sparse approach was first developed by Vanezis et al. (21), modifying the 3D visualization system of Moss et al. (23,24). Since their pioneering work, the sparse method has been developed using a geometry-based muscle modeling integrating with the facial deformation technique (26) or a flexible statistical model to reduce the facial template bias (27).

The dense approach was first introduced by Quatrehomme et al. (19) and has been modified and improved by other researchers using control data sets (28), a dense placement of soft tissue depth (29,30), a statistical shape model of both the skull and the face instead of a sole extrapolation of the deformation field (31), or computed tomography (CT)-derived implicit surface representations (20).

Automated, 3D computerized FFR has exhibited some advantages over the traditional manual methods, such as increased efficiency, producing many variations for a face, and partial removal of practitioner subjectivity. However, the new approach has exposed significant disadvantages as the reconstructed faces are biased by the template or generated faces, because the template used in a facial reconstruction is usually derived from a limited database; therefore, the facial appearance of the reconstructed face will always ultimately resemble the facial template (2,20). In an attempt to reduce this limitation, researchers have collected large-scale data with different ages, sexes, and body builds (32,33) or developed a statistical average model acquired from the analysis of a whole database (27). Another shortcoming is the paucity of published accuracy and reliability studies for the computerized systems.

Another approach to the computer-generated FFR has been developed by Wilkinson (34) who introduced a "virtual sculpture" method utilizing a 3D modeling system (FreeForm Modelling Plus™; Sensable Technologies, Wilmington, MA) with haptic feedback (Phantom Desktop™ Haptic Device; Sensable Technologies). This method attempts to mimic the 3D manual methods enabling practitioner-led facial reconstruction. The skull is imported into FreeForm Plus as a stereolithography (STL) file, converted originally from Digital Imaging and Communication in Medicine (DICOM) data, or an object file translated from laser scan data. The operator is therefore able to feel the surface in detail during the process of facial reconstruction.

The first recorded accuracy study related to facial morphology prediction was produced by Von Eggeling (35) who reported little success. He employed a death mask and facial soft tissue measurements recorded from a cadaver. Two plaster casts of the skull of the cadaver were provided along with the tissue depth measurements, and two sculptors reproduced the face independently. Von Eggeling concluded that there was no resemblance between either of the two reconstructed faces or the death mask. Stadtmüller (36) reconstructed two faces from the skulls of an elderly man and a young man, using the Kollmann and Büchly (37) facial soft tissue data, and then reported that no similarities were found between the reconstructed faces and the corresponding facial photographs from the corpses. Suk (38) concluded that facial reconstruction from the skull must resort to fantasy.

In contrast, Gerasimov (15) demonstrated high accuracy for facial morphology prediction. He performed a series of experiments using 12 skulls from cadavers and asserted that all 12 reconstructions were recognizable with strong similarity when compared to photographs of the deceased. He also reported that all of the 140 facial reconstructions attempted in his laboratory were successfully identified. Snow et al. (14) carried out an accuracy study using antemortem photographs of the subjects instead of death masks or photographs of cadavers. They produced a male and female facial reconstruction and participants were then asked to match the reconstructed face to images in a face pool. The facial reconstruction of the female face scored 26% correct matching, whereas the male face scored 68%.

Vanezis et al. (21) attempted a comparison of the FFRs produced from the manual and computerized methods in a single-blind test. The results showed that both methods could be employed as a useful tool for identification. Helmer et al. (16) performed a double-blind accuracy test using 12 skulls reconstructed independently employing a manual method by two practitioners, and three assessors determined the degree of resemblance using five-point rating scale from one (great) to five (no resemblance). The result showed 50% approximate resemblance (scale of three) as the mean rating.

Research into the reliability of FFRs has continued in the 21st century. Stephan and Henneberg (11) investigated facial morphology prediction using 16 reconstructed faces and 37 assessors. They stated that "facial approximation" should be considered highly inaccurate and unreliable, as only one facial reconstruction showed true positive identification at above chance rate, and 403 incorrect identifications were made in 592 identification scenarios. On the contrary, Wilkinson and Whittaker (17) demonstrated more optimistic results for facial morphology prediction. Employing five juvenile female forensic cases (from the West serial murder investigation in Gloucester, U.K.) facial reconstructions were produced manually and then were compared with a face pool by 50 volunteers. The participants were asked to select a face from the face pool that most resembled each reconstruction. The results showed that the mean hit rate was 44%, and all hit rates were above chance (10%). The authors concluded that facial reconstruction can produce a good resemblance to an individual.

More recently, Quatrehomme et al. (18) performed an accuracy study using 25 3D FFRs produced from a manual method employing skulls donated by the decedents. The subjects were divided into three groups, and then, each group was reconstructed by either of the two scientists who have a different degree of experiences in the field of FFR. During reconstructing the faces, the scientists were given discriminative information on the forensic analysis of the skulls. The results suggested that resemblance rates were improved in proportion to the experience of practitioners and the amount of available information from the analysis of the skulls.

Facial morphology prediction studies for computer-generated facial reconstructions have been performed recently by researchers and presented promising results. Wilkinson et al. (39) produced FFRs from two CT scanned skulls by utilizing a 3D computerized modeling system. Two face pools composed of the five facial CT scanned images including the target individual were prepared for a matching task. The assessors were asked to choose the face from the face pool that most resembled each reconstruction. The results demonstrated that the combined hit rate was 50% above the level recorded by chance (20%). The researchers also reported another pioneering study in the same article into a quantitative comparison of the facial morphology between the facial reconstruction and the facial scan of the identified individual using reverse modeling software. The results showed that the computer-generated facial reconstructions also have good levels of quantitative accuracy in relation to facial morphology prediction.

Claes et al. (27) attempted to evaluate the accuracy and identification success rate from facial reconstructions issuing from automated computerized systems employing combined statistical models. Results showed an average of 1.14-mm deviation between the scanned target and the computer-generated face, and the identification rate was 100% (based on Euclidean distance matrix

signatures of the facial surfaces in the database of 118 individuals). Identification success rate was demonstrated to be 81% when employing a face pool comparison with 28 participants.

Although some researchers have maintained that the prediction ability of FFR is unreliable, much of the previous research has shown an acceptable prediction level for recognition or identification. Also a number of forensic cases have shown that the technique of FFR can be used to assist in the identification of individuals from unknown skulls (3,5,12–14,40–44). According to these studies and forensic case reports, it could be suggested that FFR can be employed as an effective forensic tool especially when other means of identification have failed for the identification of human remains.

Average facial tissue depth data are a major contributor to the accuracy and reliability of FFR. Until present, lateral cephalometric radiographs (45,46), CT (20,25,47), magnetic resonance imaging (48,49), and ultrasound (32,50–53) have been employed to measure facial tissue depths with more accurate noninvasive analysis. Utilizing these techniques, a large amount of facial tissue depth data has been collected from various ethnic groups relating to sex, age, and body mass index and has been applied practically to FFR. Owing to further progression of 3D medical diagnosis technology, new equipment has been modified for the purpose of collecting more accurate tissue depths. Of those, recently developed cone-beam CT (CBCT) scanner has been introduced to the study of tissue depth measurements. The CBCT enables obtaining the head image of soft and hard tissue from the subject in an upright position with less radiation doses than the typical multislice CT system (54). The 3D image of a face taken from the CBCT may also allow a comparison between the face of a subject and the facial reconstruction without the soft tissue distortion caused by gravity and body position.

This study aims to assess the accuracy of facial reconstructions generated from a computerized 3D modeling system, to explore the availability of comparison between the facial reconstruction and the corresponding face of a live subject scanned from CBCT, and to investigate the validity of facial guidelines for the FFR of Korean adults.

Materials and Methods

For the purpose of a single-blind accuracy test for FFRs, this research was carried out by two study groups in different countries, United Kingdom and Republic of Korea. The Department of Orthodontics at the School of Dentistry of the Chonnam National University (CNU) in Korea undertook the recruitment of participants and the collection of facial scan data from live subjects. The facial reconstructions and comparisons between the reconstructed faces and the scanned facial surfaces were performed by a practitioner (W-JL) in the Centre for Anatomy and Human Identification (CAHID) at the University of Dundee in the United Kingdom.

Acquisition of Facial Scan Data

Three volunteers (subjects A, B, and C) were recruited from students at the CNU in Gwangju, Korea. All volunteers had neither any experiences of orthodontic treatment or facial plastic surgery nor facial deformities. Informed consents were obtained from all subjects. This study was approved by the Institutional Review Board for the Medical Science at the CNU Hospital, Gwangju, Korea. Three-dimensional images for the skulls and head surfaces were obtained using a CBCT scanner (Alphard Vega™; Asahi Roentgen Co., Kyoto, Japan) with a voxel size of 0.39 mm and field of view (FOV) of 200 × 179 mm. The subjects were scanned to acquire 3D skull and facial images in the seated upright position with a neutral and relaxed facial expression (Figs 1 and 3*Ac–Cc*). Immediately after the completion of CT scanning, the faces of each subject were photographed from frontal, three-quarter, and profile views (Fig. 3*Aa–Ca*). To differentiate two layers of soft and hard tissues, two scales of Hounsfield units (HUs) were applied during head scanning: one for a hard tissue image with +150 to +200 HUs and another for a soft tissue image with −500 to −550 HUs. Hence, all sliced images created from the CT scanning were thresholded using HU limits to be segmented into soft or hard tissue utilizing an available visualization computer software. These images were stored as a format of DICOM files and then were transmitted electronically to the CAHID at the University of Dundee with the facial photographs of the subjects. The DICOM data of the heads were converted to STL image files using a 3D visualization computer program (Amira™ version 5.2.2; Visage Imaging, San Diego, CA) by an independent CAHID staff member. A practitioner (W-JL), with one and half years training in FFR, produced the facial reconstructions. The 3D facial scan images and the photographs of the subjects were not exposed to the practitioner until the facial reconstructions had been completed.

Preparation of the Skull Models

A 3D modeling system (FreeForm Modelling Plus™ software) was utilized for the facial reconstruction process. The system involves Phantom Desktop™ Haptic Device enabling the use of the sense of touch to handle and feel digitalized 3D data developed by Wilkinson (34). The three skull models (skulls A, B, and C) were imported into FreeForm Modelling Plus as STL files (Figs 1 and 2*A*). As the biological information relating to the three live subjects was unknown to the practitioner (except ancestry group—all were northeastern Asian), anthropological assessments for the skulls were initially carried out regarding sex and age. Skull A (Fig. 1*A*) was determined as a man and aged 20–30 years; skull B (Fig. 1*B*) was determined as female and aged 20–30 years; skull C (Fig. 1*C*) was determined as a male and aged 20–30 years. The actual ages of the subjects were provided by the CNU after completion of the facial reconstructions as 30.4 years for subject A, 27.3 years for subject B, and 27.7 years for subject C.

Facial Reconstruction

The faces of the subjects were reconstructed according to the combination method (5,13) (Fig. 2). Facial soft tissue depths data for living Korean adults was utilized (Lebedinskaya et al. [50], who employed Russian–Korean residents in a province of central Russia). The tissue depth pegs were placed onto the surface of the skull at the corresponding anatomical sites using modeling clay and scale tools to adjust the exact lengths of each peg in the FreeForm software (Fig. 2*B*). Each individual facial muscle was rebuilt as accurately as possible following anatomical guidelines. A data bank of premodeled facial muscles containing 15 major facial muscles and the parotid glands was utilized in the anatomical stage. Each muscle was imported and positioned onto the skull according to the analysis of those origins and insertions. The shape and size of the muscles were altered utilizing 3D deformation tools to customize the muscle to the target skull (Fig. 2*C*). A number of guidelines were employed to predict facial components: eyes, nose, mouth, and ears including:

- 25-mm-diameter eyeballs (55) were placed in the orbits and positioned so that the eyeball and pupil were centrally located within the orbits (4,56).

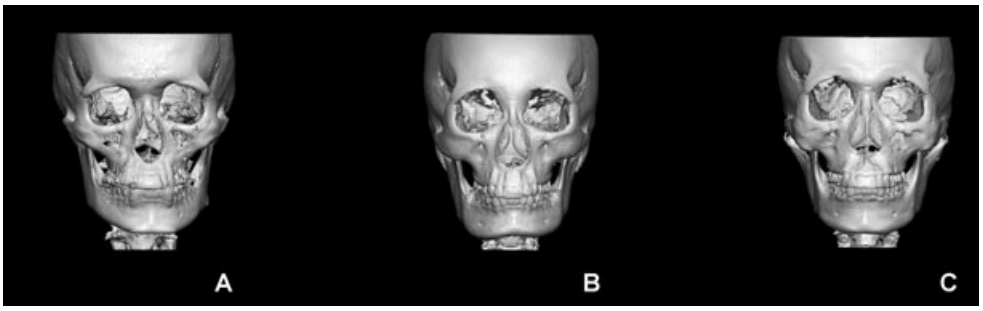

FIG. 1—*The skull models from the scans of subjects A, B, and C.*

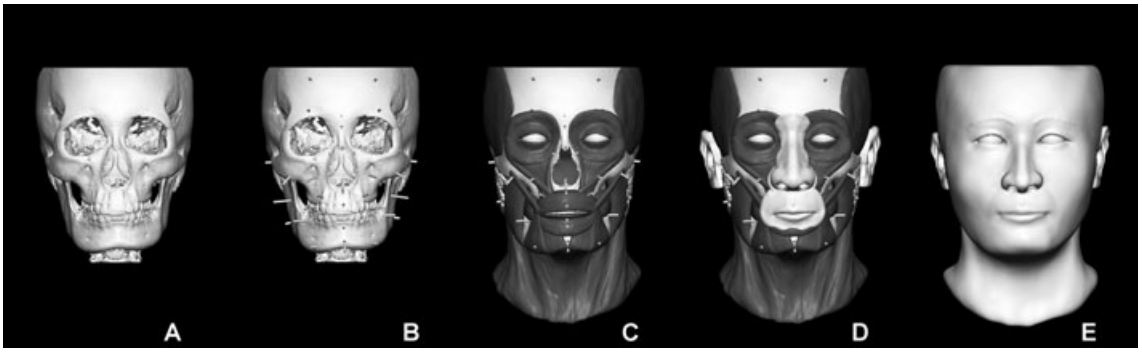

FIG. 2—*3D computerized facial reconstruction procedure following the combination method.*

- The eyeballs were positioned in the orbit so that a tangent taken from the superior to the inferior mid-orbital margins touched the iris (57).
- The inner canthus was placed 2 mm lateral to the lacrimal crest at its middle, and outer canthus can be placed 3–4 mm medial to the malar tubercle (58). Where the malar tubercle was absent, the outer canthus was positioned 10 mm below the line of the zygomatico-frontal suture and 5–7 mm from the orbital margin (58).
- The maximum width of the soft nose was estimated by that the bony nasal aperture at its widest point as three-fifths of the overall width of the soft nose (59), which has been confirmed by a CT study of living subjects regardless of ethnic group (60). The end of the soft nose was predicted as the point where a line following the projection of the portion of the nasal bones crosses a line following the direction of the nasal spine (59). The shape and size of the alae and profile of the nose were determined by the nasal aperture in profile. These prediction methods for the nose have also been confirmed using a blind study by Rynn and Wilkinson (61).
- The corners of the mouth were estimated by the maxillary canine and first premolar teeth (4,6), and sets of regression formulae derived from the positive correlation between lip thicknesses and the enamel heights of upper and lower incisors were utilized for the estimation of lip thickness (62).
- The broad length of the ears was predicted by the length of the nose (63), and the ear canal was positioned using the external auditory meatus (4). The angle of ear was set as parallel to the jaw line, and the earlobe adherence was predicted using the direction of the mastoid processes (59).

In this way, each facial component was rebuilt onto the skull (Fig. 2*D*). For the final stage of facial reconstruction, a skin layer was added over the muscle and skull structure referring to the facial anatomy and musculature by utilizing transparency tools in the FreeForm software. Finally, the FFRs were completed and displayed (Figs 2*E* and 3*Ab–Cb*).

Comparison of Facial Reconstruction and Target Face

The accuracy of the reconstructed faces was assessed using 3D morphometric surface comparison between each reconstruction and the relevant subject face. First, the FFR and corresponding CT scanned face of the subject were aligned manually in FreeForm using the embedded skull in the reconstructed face and the CT scanned head for alignment (Fig. 3*Ad–Cd*) so that the two skull models were positioned identically in dimension and orientation. Therefore, the most reliable 3D discrepancy between the facial reconstruction and the subject could be obtained. As there was a relatively large defect area on the occipital region of the subject scan, because of the limitation of FOV, the back of the head including ears and below of jaw line of both the facial reconstruction and the scanned head were removed, so that only the facial region was compared (Fig. 3*Ac–Cc*). Second, the comparison model was imported as STL files to the Geomagic Qualify software (Geomagic™ Qualify Version 10; Geomagic, Morrisville, NC) to quantitatively assess surface morphology discrepancy between the facial reconstruction and the subject. This reverse modeling software provides nine different 3D work activities and together allows high-quality polygon meshes, accurate freeform Non-Uniform Rationale B-Spline surfaces and geometrically perfect solid models to be created. Geomagic Qualify generates data as absolute mean shell deviations, SD of the errors during shell overlaps, maximum and minimum range maps, histogram plots, and finally color maps. Within the software, a shell-to-shell deviation map may be computed and automatically produced. The results include the maximum and minimum range of shell deviations, the average distance between the two shells, and

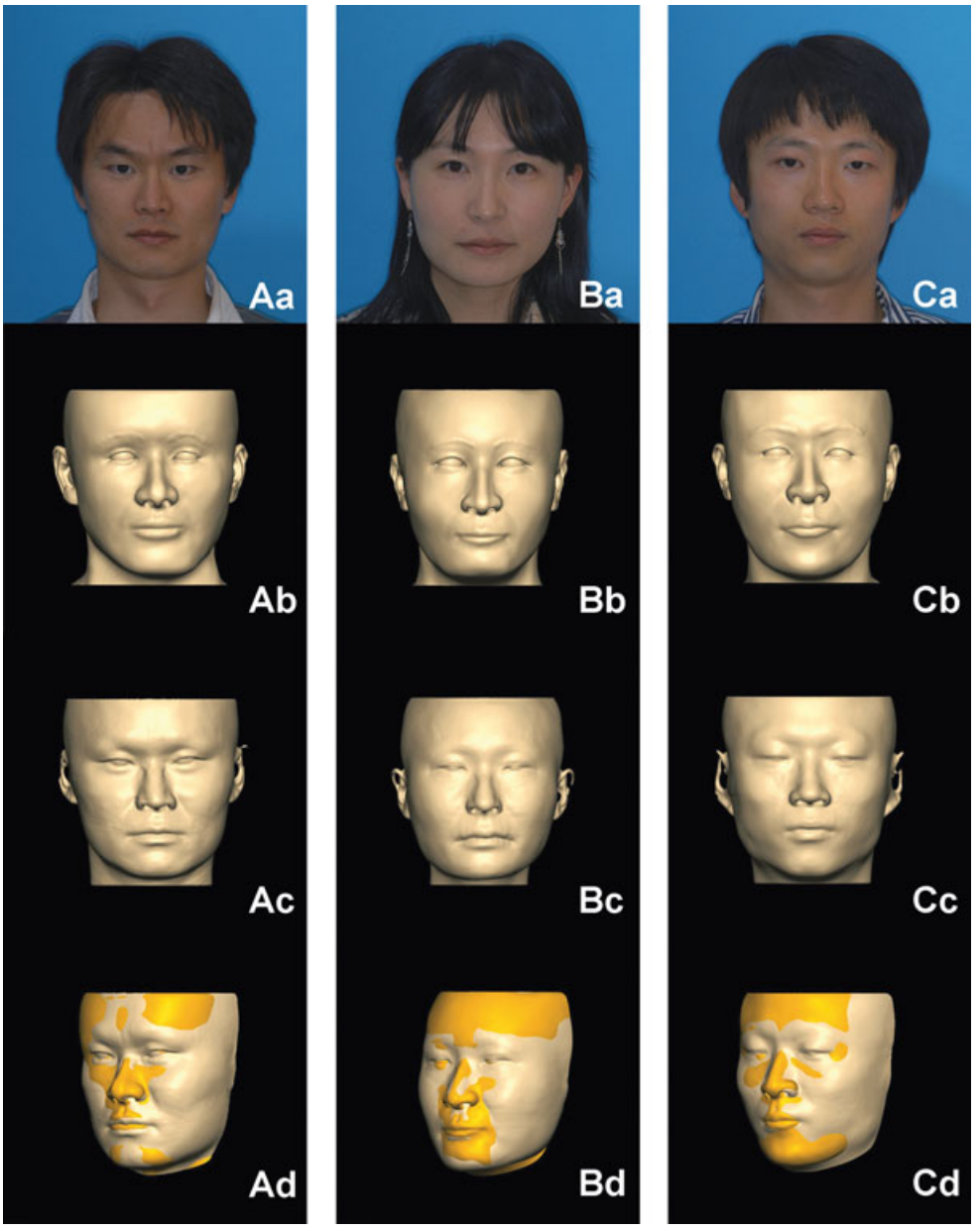

FIG. 3—*From the top row: facial photographs of subjects A, B, and C (Aa, Ba, and Ca), reconstructed faces (Ab, Bb, and Cb), scanned facial surfaces (Ac, Bc, and Cc), alignments each of the facial reconstruction, and corresponding scanned face (Ad, Bd, and Cd; gold-colored for the scanned faces, orange-colored for the reconstructions).*

the SD. This function was used to statistically analyze the differences between each facial reconstruction and the facial scan of its target.

Results

Shell-to-shell deviation maps for three comparisons between each reconstructed face and the subject face were created (Figs 4–6) and the percentage distributions for the deviations are presented in Tables 1 and 2. The discrepancies between the two shells (the errors) were computed as the minimum limit of deviation error defined within either ±2 or ±2.5 mm. The Geometric deviation maps (Figs 4–6) and tables for percentage distributions of deviations (Tables 1 and 2) were created applying ±2.5 mm of the minimum limit of deviation. In the figures, the colors on the spectrum bars and the faces of the reconstructions indicate the distribution of the errors: "green" representing the deviation of within ±1.0 mm; "yellow to red" representing from above +1.0 to +10 mm; and "darkening blue" representing from below −1.0 mm to −10 mm. The "+" (the areas of the yellow and red) implies that the skin surface of the reconstruction is more prominent than the subject face, and the "−" (the areas of the bluish color) implies that the skin surface of the reconstruction is less prominent than the subject face.

The deviation map for subject A (Fig. 4) showed that 45% of the overall surface of the reconstructed face deviated within an error ±2.0 mm in the alignment with the scanned face (Table 1), and the percentage was increased to 54% of the overall surface of the reconstructed face when the error deviation was broadened to within ±2.5 mm (Table 2). Eighty-eight percent of the facial surface was within an error ±5.0 mm (Tables 1 and 2). The averages of the error and SD were −0.46 and 2.81 mm, respectively. The most accurate areas (errors between ±1.0 mm; green-colored areas, occupied by

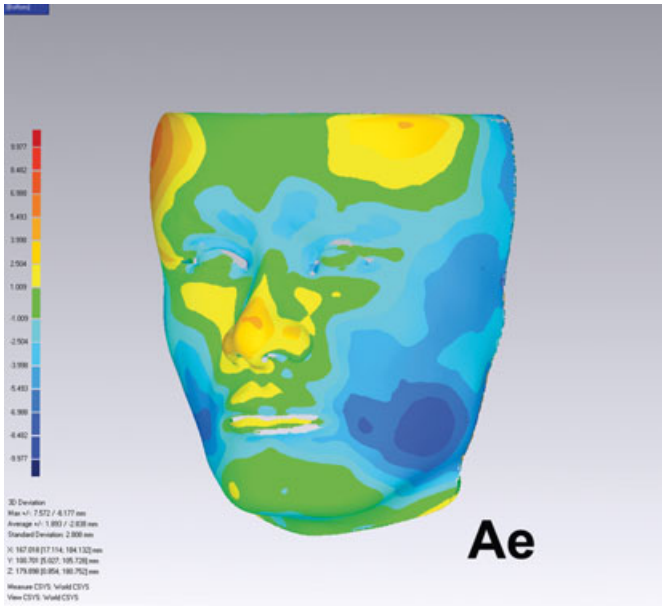

FIG. 4—*Deviation map for subject A created from morphometric comparison between the facial reconstruction and the scanned face.*

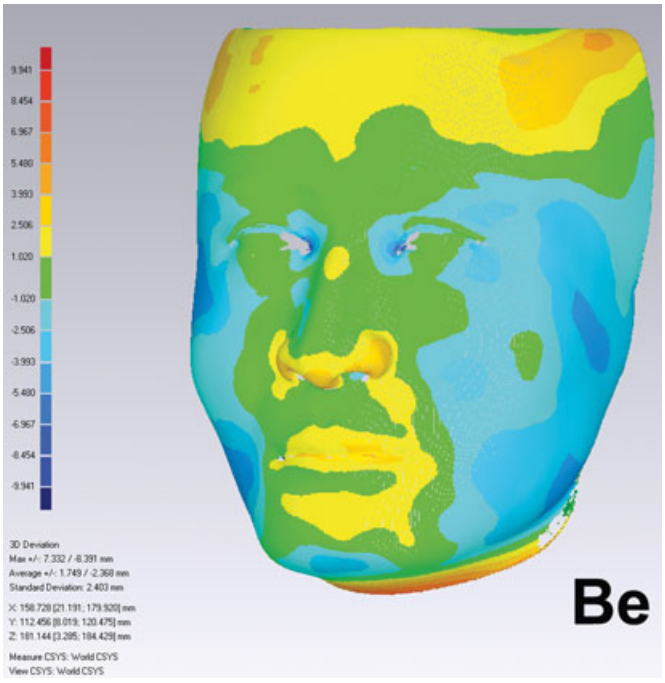

FIG. 5—*Deviation map for subject B created from morphometric comparison between the facial reconstruction and the scanned face.*

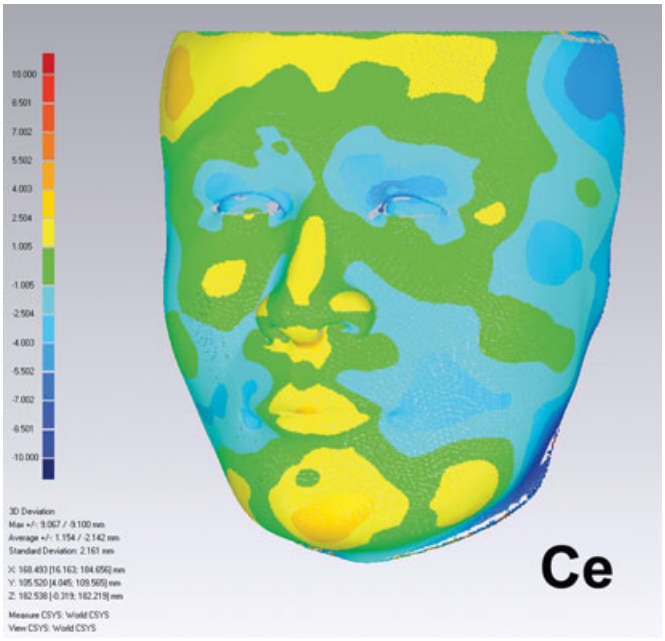

FIG. 6—*Deviation map for subject C created from morphometric comparison between the facial reconstruction and the scanned face.*

26% of the overall surface of the facial reconstruction) were found at the frontal forehead, parts of lateral forehead, eyes, both infra-orbits, nasal bridge, lateral nose, parts of the medial cheeks, philtrum, some parts of the lips, and majority of the chin. Both lateral foreheads, parts of the nasal bridge, alae, both sides of the nose, lateral and inferior portions of the nose and partial upper and lower lips, and a minor part of the chin were between +1.0 and +2.5 mm (yellow-colored areas) more prominent than the subject face. The areas around the orbits, middle of the lower forehead, both partial medial cheeks, both sides of the lips, and lateral portions of the chin were between −1.0 and −2.5 mm (light blue-colored areas) less prominent than the subject face. The largest areas of error (≥+4 and ≤−4 mm) occurred at the minor parts of the both lateral foreheads and a small part of the nose (orange-colored areas; more prominent than the subject face) and at the majority of both cheeks (dark blue-colored areas; less prominent than the subject face).

The deviation map for subject B (Fig. 5) presented that 50% of the reconstructed facial surface aligned with the scanned face within an error ±2.0 mm (Table 1), and the percentage was increased in 65% when the error deviation was broadened to within ±2.5 mm (Table 2). Ninety-seven percent of the whole surface of the facial reconstruction was within an error ±5.0 mm. The averages of the error deviation and SD were −0.31 and 2.40 mm, respectively. The most accurate areas (errors between ±1 mm; green-colored areas, occupied by 25% of the overall surface of the facial reconstruction) were at the lower forehead, eyes, eyelids, parts of the supra-orbits, infra-orbits, majority of the dorsal nose, both lateral portions of the nose, philtrum, mouth corners, and lateral chin. The majority of the frontal and lateral foreheads, parts of the nasal bridge, tip of the nose, alae, lips, and medial chin were between +1.0 and +2.5 mm (yellow-colored areas) more prominent than the subject face. Some parts of the orbits, medial and lower cheeks, and both temples and lower chin were between −1.0 and −2.5 mm (light blue-colored areas) less prominent than the subject face. The largest areas of error (≥+4 and ≤−4 mm) were found at the minor portions of the lateral foreheads (orange-colored areas; more prominent than the subject face) and at the both endocanthi and small parts of the both lateral and lower cheeks (dark blue-colored areas; less prominent than the subject face).

The deviation map for subject C (Fig. 6) revealed that 66% of the overall surface of the reconstructed face was aligned to the target face within an error ±2.0 mm (Table 1), and the proportion of the surface was increased in 77% when the error deviation was extended to within ±2.5 mm (Table 2). Ninety-five percent of the overall surface of the facial reconstruction deviated within an error ±5.0 mm in the alignment with the scanned face. The averages of the error deviation and SD were −0.49 and 2.16 mm, respectively. The most accurate areas (errors between ±1 mm; green-colored

TABLE 1—*Distribution (%) of the deviation error between the surfaces of the reconstruction and the subject within each defined error range (minimum range within ±2 mm)*

	Deviation (X: mm, minimum range within ±2 mm)					
	$-10.0 \le X < -5.0$	$-5.0 \le X < -2.0$	$-2.0 \le X \le 2.0$	$2.0 < X \le 5.0$	$5.0 < X \le 10.0$	Total (%)
Subject A	10.12	33.25 88.27	44.63	10.39	1.61	100
Subject B	2.24	32.63 97.18	50.43	14.12	0.58	100
Subject C	4.59	24.93	66.18 95.32	4.21	0.09	100

TABLE 2—*Distribution (%) of the deviation error between the surfaces of the reconstruction and the subject within each defined range (minimum range within ±2 mm).*

	Deviation (X: mm, minimum range within ±2.5 mm)					
	$-10.0 \le X < -5.0$	$-5.0 \le X < -2.5$	$-2.5 \le X \le 2.5$	$2.5 < X \le 5.0$	$5.0 < X \le 10.0$	Total (%)
Subject A	10.12	26.53 88.27	54.30	7.44	1.61	100
Subject B	2.04	25.58 97.18	64.55	7.25	0.58	100
Subject C	4.59	16.41 95.32	76.74	2.17	0.09	100

areas, occupied by 35.28% of the overall surface of the facial reconstruction) were found at the lower and lateral foreheads, both lateral orbits, infra-orbits, lateral and inferior nose, nasal tip, philtrum, upper cheeks, around the mouth, and lateral chin. The frontal forehead, nasal bridge, alae, lower tip of the nose, lips, and medial and lateral chins were between +1.0 and +2.5 mm (yellow-colored areas) more prominent than the subject face. The eyes, orbits, medial and lower cheeks, and parts of the temples were between −1.0 and −2.5 mm (light blue-colored areas) less prominent than the subject face. The largest areas of error (≥+4 and ≤−4 mm) occurred at the both endocanthi, left side of the upper eyelid, and partial temples (dark blue-colored areas; less prominent than the subject face). There was no area of the reconstructed face more prominent than the subject face with the error deviation above +4.0 mm.

Discussion

There are a number of methods in use to evaluate the accuracy of FFRs, yet the methods might be divided into two main groups: qualitative and quantitative assessments. In the early period of the accuracy studies, death masks or photographs of the deceased were compared with the reconstructed faces to determine the level of resemblance (35,36,64). These attempts can be considered as primitive qualitative studies for assessing the accuracy of facial reconstructions. Demands for more realistic *in vivo* experimentation lead to the one-to-one comparisons of the facial reconstruction with a photograph of the target individual during life (5,15,41,42). For more accurate qualitative evaluation, some researchers tested the accuracy using face pool matching (14,17,65,66). In the face pool test, the assessors were asked to match an image of the facial reconstruction to a face pool of images including the antemortem target face.

The one-to-one comparison and face pool matching are very useful methods for the assessment of the accuracy of facial reconstruction, but further objective methods were required to evaluate the accuracy quantitatively. Recently developed 3D anthropometrical software enabled the comparison of a facial reconstruction with the 3D model of the corresponding subject face or another facial reconstruction. Two 3D facial models can be aligned so that the differences in surface contours between two models can be computed numerically. Many current FFR studies have acquired facial soft- and hardtissue data from CT scans, but only a few studies have used this approach to assess the accuracy of the facial reconstruction.

In a study by Wilkinson et al. (39), CT scanned skull models from two live individuals (white North American male and female) were used for facial reconstructions. The researchers employed a 3D computer modeling system (the same one utilized in this study) and facial soft tissue depth data for white North American male and female (51) to reconstruct the faces. The accuracy of the reconstructions was assessed quantitatively using reverse modeling software (Rapidform™; Rapidform, Seoul, Korea). The results for the white man demonstrated that 60% of the reconstructed face deviated with the facial scan no more than ±2.5 mm and that the most accurate areas of the reconstruction were at the nose, chin, mouth, eyes, and left forehead. The right temple, upper cheek, ears, the nasal tip, and parts of the neck were more than 5 mm less or more prominent than the facial scan. The results for the white woman demonstrated that 52% of the reconstructed face deviated with the facial scan no more than ±2.5 mm and that the most accurate areas of the reconstruction were at the nose, chin, upper mouth, upper cheeks, and cranium. The nasal alae, lower cheeks, upper lip, and ears were between 3 and 8 mm or more than 8 mm more prominent than the facial scan.

The results of this study are comparable to those of Wilkinson et al. (39) whose research demonstrated that 60% for the male face and 52% for the female face were in the deviation within ±2.5 mm, and 90% for the male and 75% of the female were in the deviation between ±5.0 mm. Considering the overall deviation errors between the reconstructions and the scanned faces from this study with the results from the previous research by Wilkinson et al. (39), we conclude that the 3D computerized facial reconstruction system is capable of reliable facial prediction. However, it

must be acknowledged that this study is small, and even when combined with the previous study (39), the total number of subjects (n = 5) is not sufficient to reach any firm conclusions regarding reliability.

The average errors and SD between the surfaces of the reconstructions and subjects were −0.46 and 2.81 mm for subject A, −0.31 and 2.40 mm for subject B, and −0.49 and 2.16 mm for subject C. Claes et al. (27) carried out a series of accuracy tests for the 118 facial reconstructions generated from an automated computerized FFR system using a flexible statistical model. The researcher reported a result that the overall average absolute reconstruction error and SD between the reconstructed skin surface and the real test skin surface are 1.14 and 1.04 mm, respectively. This study showed lower errors than the result from the study of Claes et al. (27) and may suggest that the 3D computerized modeling method for FFR enables to reconstruct the face more accurately than the automated system. Moreover, contrasting with the recently updated data in the research of Claes et al. (27), the average facial soft tissue depths for adult Koreans used in this project (50) was obtained from the Korean population group who had emigrated from Korea to central Russia 80 years ago and have resided in the region with little interchange of people between the group in Russia and the majority in Korea. Even though the population has maintained a homogeneous ethnicity after the emigration, different climates, diet, and lifestyle might affect facial tissues. Indeed, the cheeks of all the target faces were more prominent than the reconstructions (Figs 3*Ad–Cd* and 4–6). The results may imply that the tissue depth data from the study of Lebedinskaya et al. (50) are not wholly appropriate for current Korean adults and that further research to update the data using contemporary population group is required. The under- or overestimation of the tissue depths may also be a reflection of variation related to occlusion and facial type (51) and highlights one of the problems associated with a small sample size of three subjects. Despite the differences at the cheeks, the errors recorded for the reconstructions were similar to those recorded in previous research (39).

There are other considerations when comparing this research to the previous study. Wilkinson et al. (39) utilized a conventional spiral CT scanner in which the subject is required to be in supine position. The position may cause gravity effects on the cheek and mouth areas of the face to sag downward, whereas they employ the facial tissue depth data taken from upright subjects (52). This positional difference may explain the fuller cheeks, more prominent upper lips and ear pattern errors seen for the reconstructions when compared to the facial scans. The current study employed CBCT to acquire the soft and hard tissue scan data for the subjects, which allows the face to be in upright position eliminating the possible distortions of the facial soft tissue caused by the gravity with lower radiation doses (55).

However, there is a limit to the FOV in CBCT (the FOV was 200 × 179 mm in this study) resulting in an inability to scan the whole head and an unnecessary artifact on the back of the scanned head. Nevertheless, it is thought that the excluded portions would not influence the reconstruction errors because the adult tissue depths at these areas show a constant thickness regardless of age, sex, and ancestry (67–71) and are relatively unproblematic to rebuild. Therefore, it is possible that the reconstruction error would decrease rather than to increase if the rest of the head were included and compared.

The prediction of the location, size, and morphology of facial features—eyes, nose, mouth, and ears—is critical to the level of the accuracy of FFR. The greater part of the feature prediction is based on analysis of the relation between skull structures and soft tissue components, and a number of guidelines have been introduced. However, as there is a paucity of research into determining facial features of Koreans or other northeastern Asians, this research applied guidelines derived from white European or black African populations. Figures 3–6 show that all the facial features demonstrated very low error deviations and a good likeness to the subject except the mouth position for subject A. From these results, it can be concluded that the preexisting guidelines are applicable to reconstruct the face of northeastern Asians, but also further studies are demanded to produce more accurate prediction methods from diverse ethnic groups.

Currently CBCT scanning has been used in the field of orthodontics and maxillofacial surgery (72–74). The CBCT enables to collect image data from the subjects in an upright position rather than supine position, and it is reported that radiation dose in CBCT scan is much less than multislice CT (75–77). These advantages over the conventional spiral CT and other diagnostic imaging devices can be modified for the purpose of measuring facial skin thicknesses and scanning facial surface. The results from this study present good examples to demonstrate the usefulness of the CBCT in accuracy tests of the facial reconstruction. In addition, the CBCT has a great potentiality in tissue depth measurements as once the scanned images are obtained, the measurements can be repeated, and an unlimited number of measurements can be added according to the research requirements. Because of the advances in the technology of diagnostic imaging software integrating with CBCT, scanned images can contribute to allow displaying soft and hard tissue images simultaneously on a computer screen. Some researchers have started to use the CBCT in FFR (55), and it is expected that further research employing the CBCT will be carried out in the domain of FFR.

The 3D computer modeling system (FreeForm Modelling Plus™) with haptic feedback (Phantom Desktop™) has involved actively not only in computer-generated FFRs but also in forensic investigations to simulate an incidence with engaging our tactile senses to shape and manipulate digitized 3D models in a noninvasive manner (78). Some of the strengths of the system for the FFR are that muscles, layer by layer, and skin can be visualized as separate units, with the ''transparency'' tool—a process not available in the manual method, and the simultaneous visibility of multilayers might allow alignment of two reference objects (the skull images in this study) to assess the accuracy. This method is also reproducible, quick, and provides little or no damage to the original specimen. The additions of skin texture, eyelid position, and hairstyle, as well as altering degrees of facial tissue depth are quicker and easier to integrate with animation or other computerized programs. Because of the merits, demands for computerized modeling have increased, especially in historical or archaeological facial reconstructions where realistic facial depictions are required (3,79,80). Consequently, this computer facial reconstruction system can be applied widely and reliably to forensic identification investigation.

Conclusions

The results from this study demonstrate that this computerized 3D modeling method is capable of producing reliable facial reconstructions with acceptable levels of resemblance employing the combination method and the images scanned from CBCT. This study also suggests that previously published guidelines for the prediction of facial features are applicable to the reconstruction of adult Korean faces. However, further research is recommended to update Korean tissue depth data and to examine feature prediction standards in relation to northeastern Asians in order to increase the accuracy of craniofacial reconstruction in this demographic.

References

1. Stephan CN. Anthropological facial 'reconstruction'—recognizing the fallacies, 'unembracing' the errors, and realizing method limits. Sci Justice 2003;43(4):193–200.
2. Wilkinson CM. Computerized forensic facial reconstruction: a review of current systems. Forensic Sci Med Pathol 2005;1(3):173–7.
3. Wilkinson CM. Facial reconstruction—anatomical art or artistic anatomy? J Anat 2010;216(2):235–50.
4. Krogman WM, İşcan MY. The human skeleton in forensic medicine, 2nd edn. Springfield, IL: Charles C. Thomas, 1986.
5. Prag J, Neave RAH. Making faces. London, UK: British Museum Press, 1997.
6. George RM. Anatomical and artistic guidelines for forensic facial reconstruction. In: İşcan MY, Helmer RP, editors. Forensic analysis of the skull. New York, NY: Wiley-Liss, 1993;215–27.
7. Kunstkamera. Face of our ancestors: an exhibition on the occasion of Mikhail Gerasimov's centenary, 1998, http://www.kunstkamera.ru/en/temporary_exhibitions/virtual/gerasimov/03/the_predecessors (accessed April 12, 2010).
8. Wilkinson CM, Neave RAH. The reconstruction of a face showing a healed wound. J Arch Sci 2003;30(10):1343–8.
9. Ubelaker DH, O' Donnell G. Computer-assisted facial reproduction. J Forensic Sci 1992;37(1):155–62.
10. Wilkinson CM. Facial anthropology and reconstruction. In: Thompson TJU, Black SM, editors. Forensic human identification: an introduction. Boca Raton, FL: CRC Press Inc., 2007;231–56.
11. Stephan CN, Henneberg M. Building faces from dry skulls: are they recognized above chance rates? J Forensic Sci 2001;46(3):432–40.
12. Taylor KT. Forensic art and illustration. Boca Raton, FL: CRC Press, 2001.
13. Wilkinson CM. Forensic facial reconstruction. Cambridge, UK: Cambridge University Press, 2004.
14. Snow CC, Gatliff BP, McWilliams KR. Reconstruction of facial features from the skull: an evaluation of its usefulness in forensic anthropology. Am J Phys Anthropol 1970;33(2):221–8.
15. Gerasimov MM. The face finder. New York, NY: Lippincott, 1971.
16. Helmer RP, Röhricht S, Petersen D, Möhr F. Assessment of the reliability of facial reconstruction. In: İşcan MY, Helmer RP, editors. Forensic analysis of the skull: craniofacial analysis, reconstruction, and identification. New York, NY: Wiley Liss Publishers, 1993;75–83.
17. Wilkinson CM, Whittaker DK. Juvenile forensic facial reconstruction: a detailed accuracy study. Proceedings of the 10th Conference of the International Association of Craniofacial Identification; 2002 Sept 11–14. Bari, Italy: University of Bari Press, 2002;11–4.
18. Quatrehomme G, Balaguer T, Staccini P, Alunni-Perret V. Assessment of the accuracy of three-dimensional manual craniofacial reconstruction: a series of 25 controlled cases. Int J Legal Med 2007;121(6):469–75.
19. Quatrehomme G, Cotin S, Subsol G, Delingette H, Garidel Y, Grévin G, et al. A fully three-dimensional method for facial reconstruction based on deformable models. J Forensic Sci 1997;42(4):649–52.
20. Vandermeulen D, Claes P, Loeckx D, De Greef S, Willems G, Suetens P. Computerized craniofacial reconstruction using CT-derived implicit surface representations. Forensic Sci Int 2006;159(1):164–74.
21. Vanezis P, Blowes RW, Linney AD, Tan AC, Richards R, Neave R. Application of 3-D computer graphics for facial reconstruction and comparison with sculpting techniques. Forensic Sci Int 1989;42(1–2):69–84.
22. Evenhouse R, Rasmussen M, Sadler L. Computer-aided forensic facial reconstruction. J Biocommun 1992;19(2):22–8.
23. Moss JP, Linney AD, Grindrod SR, Arridge SR, Clifton JS. Three-dimensional visualization of the face and skull using computerized tomography and laser scanning techniques. Eur J Orthod 1987;9(4):247–53.
24. Moss JP, Linney AD, Grindrod SR, Mosse CA. A laser scanning system for the measurement of facial surface morphology. Opt Lasers Eng 1989;10(3–4):179–90.
25. Tilotta F, Richard F, Glaunès J, Berar M, Gey S, Verdeille S, et al. Construction and analysis of a head CT-scan database for craniofacial reconstruction. Forensic Sci Int 2009;191(1–3):112.e1–e12.
26. Kähler K, Haber J, Seidel H-P. Reanimating the dead: reconstruction of expressive faces from skull data. ACM Trans Graph 2003;22(3):554–61.
27. Claes P, Vandermeulen D, De Greef S, Willems G, Suetens P. Craniofacial reconstruction using a combined statistical model of face shape and soft tissue depths: methodology and validation. Forensic Sci Int 2006;159(Suppl):S147–58.
28. Nelson LA, Michael SD. The application of volume deformation to three-dimensional facial reconstruction: a comparison with previous techniques. Forensic Sci Int 1998;94(3):167–81.
29. Turner WD, Brown REB, Kelliher TP, Tu PH, Taister MA, Miller KWP. A novel method of automated skull registration for forensic facial approximation. Forensic Sci Int 2005;154(2–3):149–58.
30. Pei Y, Zha H, Yuan Z. The craniofacial reconstruction from the local structural diversity of skulls. Comput Graph Forum 2008;27(7):1711–8.
31. Berar M, Desvignes M, Bailly G, Payan Y. 3D semi-landmarks-based statistical face reconstruction. J Comp Info Technol 2006;14(1):31–43.
32. De Greef S, Claes P, Mollemans W, Loubele M, Vandermeulen D, Suetens P, et al. Semi-automated ultrasound facial soft tissue depth registration: method and validation. J Forensic Sci 2005;50(6):1282–8.
33. De Greef S, Claes P, Vandermeulen D, Mollemans W, Suetens P, Willems G. Large-scale in-vivo Caucasian facial soft tissue thickness database for craniofacial reconstruction. Forensic Sci Int 2006;159(1):S126–46.
34. Wilkinson CM. Virtual sculpture as a method of computerized facial reconstruction. Proceedings of the 1st International Conference on Reconstruction of Soft Facial Parts; 2003 March 17–18; Potsdam, Germany. Remagen, Germany: Kreartive Konzepte, Beate Surek, 2003;59–63.
35. Von Eggeling H. Die leistungsfahigkeit physiognomischerrekon-struktionsversuche auf grundlagc des schädels. Arch Anthropol 1913;12:44–7.
36. Stadtmüller F. Zur beurteilung der plastischen rekonstruktionsmethode der physiognomie auf dem schädel. J Morphol Anthropol 1922;22:337–72.
37. Kollmann J, Büchly W. Die persistenz der rassen und die reconstruction der physiognomie prahistorischer schädels. Arch Anthropol 1898;25:329–59.
38. Suk V. Fallacies of anthropological identifications. Publications de la Facultae des sciences de l'Universitae Masaryk 1935;207:3–18.
39. Wilkinson C, Rynn C, Peters H, Taister M, Kau CH, Richmond S. A blind accuracy assessment of computer-modeled forensic facial reconstruction using computed tomography data from live subjects. Forensic Sci Med Pathol 2006;2(3):179–88.
40. Suzuki T. Reconstitution of a skull. Int Crim Police Rev 1973;264:76–80.
41. Gatliff BP, Snow CC. From skull to visage. J Biocommun 1979;6(2):27–30.
42. Haglund WD, Reay DT. Use of facial approximation techniques in identification of Green River Serial Murder victims. Am J Forensic Med Pathol 1991;12(2):132–42.
43. Vanezis P, Vanezis M, McCombe G., Niblett T. Facial reconstruction using 3-D computer graphics. Forensic Sci Int 2000;108(2):81–95.
44. Wilkinson C, Neave RAH. Skull re-assembly and the implications for forensic facial reconstruction. Sci Justice 2001;41(3):233–4.
45. George RM. The lateral craniographic method of facial reconstruction. J Forensic Sci 1987;32(5):1305–30.
46. Utsuno H, Kageyama T, Deguchi T, Umemura Y, Yoshino M, Nakamura H, et al. Facial soft tissue thickness in skeletal type I Japanese children. Forensic Sci Int 2007;172(2–3):137–43.
47. Kim KD, Ruprecht A, Wang G, Lee JB, Dawson DV, Vannier MW. Accuracy of facial soft tissue thickness measurements in personal computer-based multiplanar reconstructed computed tomographic images. Forensic Sci Int 2005;155(1):28–34.
48. Sahni D, Jit I, Gupta M, Singh P, Suri S, Sanjeev S. Preliminary study on facial soft tissue thickness by magnetic resonance imaging in northwest Indians. Forensic Sci Commun 2002;4:1–7.
49. Sahni D, Sanjeev S, Singh G, Jit I, Singh P. Facial soft tissue thickness in northwest Indian adults. Forensic Sci Int 2008;176(2–3):137–46.
50. Lebedinskaya GV, Balueva TS, Veselovaskaya VS. Principles of facial reconstruction. In: İşcan MY, Helmer RP, editors. Forensic analysis of the skull: craniofacial analysis, reconstruction and identification. New York, NY: Wiley, 1993;183–98.
51. Utsuno H, Kageyama T, Uchida K, Yoshino M, Miyazawa M, Inoue K. Facial soft tissue thickness in Japanese children. Forensic Sci Int 2010;199(1):109e1–e6.
52. Manhein MH, Listi GA, Barsley RE, Musselman R, Barrow NE, Ubelaker DH. In vivo facial tissue depth measurements for children and adults. J Forensic Sci 2000;45(1):48–60.
53. Wilkinson CM. In vivo facial tissue depth measurements for white British children. J Forensic Sci 2002;47(3):459–65.
54. Smith SL, Throckmorton GS. A new technique for three-dimensional ultrasound scanning of facial tissues. J Forensic Sci 2004;49(3):451–7.
55. Fourie Z, Damstra J, Gerrits PO, Ren Y. Accuracy and reliability of facial soft tissue depth measurements using cone beam computer tomography. Forensic Sci Int 2010;199(1–3):9–14.
56. Tian S, Nishida Y, Isberg B, Lennerstrand G. MRI measurements of normal extraocular muscles and other orbital structures. Graefes Arch Clin Exp Ophthalmol 2000;238(5):393–404.

57. Gatliff BP. Facial sculpture on the skull for identification. Am J Forensic Med Pathol 1984;5(4):327–32.
58. Wilkinson CM, Mautner SA. Measurement of eyeball protrusion and its application in facial reconstruction. J Forensic Sci 2003;48(1):12–6.
59. Gerasimov MM. Facial reconstruction from the cranium. Translator Tshernezky W, Moscow, Russia: Izdat. Akademii Nauk SSSR, 1955.
60. Angel JL. Restoration of head and face for identification. Proceedings of the 30th Annual Meeting of the American Academy of Forensic Sciences; 1987 Feb 20-25; St. Louis, MO. Colorado Springs, CO: American Academy of Forensic Sciences, 1987.
61. Rynn C, Wilkinson CM. Appraisal of traditional and recently proposed relationships between the hard and soft dimensions of the nose in profile. Am J Phys Anthropol 2006;130(3):364–73.
62. Rynn C, Wilkinson CM, Peters HL. Prediction of nasal morphology from the skull. Forensic Sci Med Pathol 2009;6(1):1–15.
63. Wilkinson CM, Motwani M, Chiang E. The relationship between the soft tissues and the skeletal detail of the mouth. J Forensic Sci 2003;48(4):728–32.
64. Fedosyutkin BA, Nainys JV. The relationship of skull morphology to facial features. In: İşcan MY, Helmer RP, editors. Forensic analysis of the skull. New York, NY: Wiley-Liss, 1993;199–213.
65. Wilder HH, Wentwoith B. Personal identification. Boston, MA: Gormon Press, 1918.
66. Stephan CN, Henneberg M. Recognition by forensic facial approximation: case specific examples and empirical tests. Forensic Sci Int 2005;156(2–3):182–91.
67. Rhine JS, Campbell HR. Thickness of facial tissues in American blacks. J Forensic Sci 1980;25(4):847–58.
68. Helmer R. Schädelidentifizierung durch elektronische bildmischung. Heidelberg, Germany: Kriminalistik Verlag GmbH, 1984.
69. Phillips VM, Smuts NA. Facial reconstruction: utilization of computerized tomography to measure facial tissue thickness in a mixed racial population. Forensic Sci Int 1996;83(1):51–9.
70. Stephan CN, Simpson EK. Facial soft tissue depths in craniofacial identification (part I): an analytical review of the published adult data. J Forensic Sci 2008;53(6):1257–72.
71. Tedeschi-Oliveira SV, Melani RFH, de Almeida NH, de Paiva LAS. Facial soft tissue thickness of Brazilian adults. Forensic Sci Int 2009;193(1–3):127e1–e7.
72. Kau CH, Richmond S, Palomo JM, Hans MG. Three-dimensional cone beam computerized tomography in orthodontics. J Orthod 2005;32(4):282–93.
73. Hechler SL. Cone-beam CT: applications in orthodontics. Dent Clin North Am 2008;52(4):809–23.
74 Cattaneo PM, Melsen B. The use of cone-beam computed tomography in an orthodontic department in between research and daily clinic. World J Orthod 2008;9(3):269–82.
75. Mah JK, Danforth RA, Bumann A, Hatcher D. Radiation absorbed in maxillofacial imaging with a new dental computed tomography device. Oral Surg Oral Med Oral Pathol Oral Radiol Endod 2003;96(4):508–13.
76. Tsiklakis K, Donta C, Gavala S, Karayianni K, Kamenopoulou V, Hourdakis CJ. Dose reduction in maxillofacial imaging using low dose cone beam CT. Eur J Radiol 2005;56(3):413–7.
77. Swennen GR, Schutyser F. Three-dimensional cephalometry: spiral multi-slice vs cone-beam computed tomography. Am J Orthod Dentofacial Orthop 2006;130(3):410–6.
78. Buck U, Naether S, Braun M, Thali M. Haptics in forensics: the possibilities and advantages in using the haptic device for reconstruction approaches in forensic science. Forensic Sci Int 2008;180(2–3):86–92.
79. Benazzi S, Fantini M, De Crescenzio F, Mallegni G, Mallegni F, Persiani F, et al. The face of the poet Dante Alighieri reconstructed by virtual modelling and forensic anthropology techniques. J Arch Sci 2009;36(2):278–83.
80. Benazzi S, Stansfield E, Milani C, Gruppioni G. Geometric morphometric methods for three-dimensional virtual reconstruction of a fragmented cranium: the case of Angelo Poliziano. Int J Legal Med 2009;123(4):333–44.

Additional information and reprint requests:
Caroline M. Wilkinson, Ph.D.
Centre for Anatomy and Human Identification
College of Life Sciences
University of Dundee
MSI/WTB Complex
Dow Street
Dundee DD1 5EH
U.K.
E-mail: c.m.wilkinson@dundee.ac.uk